24.1 A Long-Range Narrowband RF Localization System with a Crystal-Less Frequency-Hopping Receiver

Chien-Wei Tseng[1], Demba Komma[1], Kuan-Yu Chen[1], Rohit Rothe[1], Zhen Feng[1], Makoto Yasuda[2], Masaru Kawaminami[3], Hun-Seok Kim[1], David Blaauw[1]

[1]University of Michigan, Ann Arbor, MI
[2]United Semiconductor Japan, Kuwana, Japan
[3]United Semiconductor Japan, Yokohama, Japan

Emerging IoT applications, such as asset tracking and first-responder rescue operation, require a new localization solution that achieves decimeter-level accuracy for long range (km) in GPS-denied indoor non-line-of-sight (NLOS) scenarios. Impulse-response ultra-wideband radar (IR-UWB) [1-3] can achieve high precision, but cannot operate in long distance NLOS conditions due to FCC-regulated transmit-power limits and severe pathloss through walls. Moreover, IR-UWB requires very high instantaneous power (> 70mW [2]) rendering it impractical for energy-constrained IoT with small batteries and high internal resistance. Lower-power solutions with narrower bandwidth, based on WiFi [4] or Bluetooth [5], typically have a limited range of < 100m or are not operable in NLOS. A proprietary 80MHz OFDM-based solution [6] using an active-reflection IC achieved decimeter-level accuracy in NLOS conditions. However, it requires relatively high power consumption (62.8mW) with a limited range up to ~100m. Addressing this technological gap, we propose a new crystal-less low-power RF receiver with -115dBm sensitivity for long-distance (up to 483m) ranging in NLOS conditions with decimeter-level (~0.6m) accuracy.

The proposed receiver uses a free-running oscillator to coherently demodulate frequency-hopping narrowband (3kHz) OFDMA symbols concurrently transmitted from main and reflecting anchors as shown in Fig. 24.1.1. The narrow band of each individual OFDMA subcarrier symbols provides a high sensitivity of -115dBm, resulting in a long range (up to 483m), whereas high accuracy (~0.6m) is attained by utilizing a relatively wide bandwidth (100MHz) in the 2.4GHz band, covered by 512 frequency hops. The proposed PLL-less design without an RF-reference crystal lowers the power consumption as well as the cost of the tag. However, it inevitably invites substantial phase noise and frequency drift from a free-running LC-oscillator. We mitigate this issue with novel baseband symbol-stitching using strategically placed pilot subcarriers to estimate and compensate the phase offset and frequency drift of the LO. As a result, the system demonstrates: 1) low-power and low-cost design without a PLL or crystal traditionally used for coherent OFDMA demodulation, 2) high sensitivity (long distance) reception of time-multiplexed narrowband subcarriers, and 3) high-resolution channel impulse response (CIR) and time-difference-of-arrival (TDoA) estimation from the OFDMA waveform that spans 100MHz bandwidth.

The localization system, shown in Fig. 24.1.1, consists of one main anchor, multiple reflecting anchors (two shown) and multiple tag receivers (one shown). The main anchor simultaneously transmits a 5.8GHz signal to the reflecting anchors and a 2.4GHz signal directly to the tag. The reflecting anchors relay (or reflect) the incoming 5.8GHz signal from the main anchor to the tag after shifting it to the 2.4GHz band and adding a small (50kHz) anchor-specific OFDMA subcarrier shift. The tag receives the combination of the subcarrier signals transmitted simultaneously by the anchors, each occupying an orthogonal frequency of 3kHz bandwidth. The main anchor hops sequentially through the selected subcarrier (200kHz step, skipping unused subcarriers) until the full localization bandwidth (100MHz) is sparsely covered. The tag performs a coordinated frequency hopping of its own to receive and stitch all OFDMA subcarrier symbols in a phase-coherent manner and obtain the channel frequency responses (CFRs) for all anchors over the 100MHz bandwidth. The TDoA is the time difference between the CIR (i.e., IFFT of CFR) of different anchors. Finally, TDoA trilateration with known anchor positions provides the estimated tag location.

Figure 24.1.2 shows the crystal-less frequency-hop receiver and pilot-assisted phase recovery scheme. The tag receives 512 time-multiplexed subcarrier symbols over 100MHz bandwidth. However, a 100MHz bandwidth receiver would result in high power consumption by requiring a wide-bandwidth LNA and high-frequency baseband and also open the receiver to out-of-band interference due to limited frequency filtering. Instead, we take advantage of the fact that only a narrow bandwidth is in use at any time. We therefore propose a narrow 2MHz bandwidth receiver which sequentially shifts its RF LO frequency with 2MHz steps and receives 10 time-multiplexed OFDMA symbols that are 200kHz apart per iteration. As a result, we benefit from the efficiency of a narrow-band receiver but, by LO frequency hopping and synchronized input-matching adjustment, the receiver covers the 100MHz bandwidth necessary for high-precision CIR/TDoA estimation. Since the receiver uses a free-running LO without a PLL to reduce cost and power, it exhibits relatively poor phase noise and frequency drift that are unacceptable to coherently receive OFDMA symbols. We mitigate this issue with 1) pilot-assisted frequency-drift and phase-noise compensation, and 2) pilot-phase alignment using an overlapping symbol between two adjacent windows, both performed in baseband (off-chip in our implementation). We first perform off-line, single-shot calibration for the LO to acquire the window-frequency control code, which does not need to be very accurate as long as the OFDMA symbols are encompassed within the 0.4-to-3MHz IF window bandwidth. The IF bandwidth is chosen to allow an additional (11th) overlapping symbol and 400kHz window margin to account for voltage/temperature variations (Fig. 24.1.2, top, left and Fig. 24.1.3 bottom right). In addition to 10+1 hopping symbols transmitted during one 2.2MHz IF window, the main anchor transmits a pilot subcarrier with a constant phase as shown in Fig. 24.1.2 (left). This pilot allows the tag to directly observe the frequency offset as well as the phase noise during 10+1 hopping symbols for an IF window. The observed phase noise and frequency offset are then later cancelled during the CFR stitching process. However, when the receiver shifts the LO frequency for the next window, the phase coherency of the pilot is not maintained. To recover the pilot phase after a window shift, the main anchor sends the last symbol in the IF window for twice the regular duration so this continuous, double-length symbol is received in both IF windows (Fig. 24.1.2, left). By matching the phase between the overlapping symbols received in the two windows, we recover the phase of the new pilot and coherently stitch all windows over the entire 100MHz bandwidth for CFR / CIR estimation.

Figure 24.1.3 presents the narrowband, crystal-less, low-IF I/Q tag receiver architecture, featuring synchronously adjusted input matching and LO frequency. The narrowband input matching is enabled by a fixed, off-chip, high-Q (> 50) inductor (3nH) and capacitor (0.5pF) tuned with a (20-to-100fF) 5-bit switched-cap array (SCA) to adjust the center frequency. The LNA is designed with a conventional inductive-degeneration topology to achieve narrowband performance. The continuous pilot tone calibrates the LO phase noise and eliminates the need for a power-consuming phase-locked loop and high-performance oscillator. Also, to accommodate 50 IF window shifts to cover the 100MHz localization bandwidth, fast LO settling between hops is essential. Therefore, a free-running LC oscillator with 15-bit SCA topology is chosen to achieve the target frequency shift with fast, 0.3us frequency settling, in measurement. The frequency-control words of the SCA are off-line measured by a frequency counter (Keysight 53220A) and stored back in the frequency hop table in the digital controller for a one-time calibration. The measured frequency resolution of the oscillator is ~80kHz over the entire localization bandwidth.

The proposed tag receiver was fabricated in 55nm DDC process technology provided by United Semiconductor Japan CO., Ltd. The die micrograph is shown in Fig. 24.1.7 and occupies 0.85mm^2. Figure 24.1.4 shows the measurement of the receiver's performance. The free-running oscillator achieves 0.3□s average frequency-shift settling time for the required 4MHz hop, and a phase noise of -85dBc/Hz at 100kHz offset is measured under 800uA at 4.9GHz frequency. The total front-end receiver consumes 3.9mW under 0.9V supply. The receiver can support three gain modes (52dB, 46dB, 40dB) with noise figure around 6.5dB in high-gain mode. Three input matching settings are selected to change along with IF window shifts.

Figure 24.1.5 shows the measurement setup and the TDoA ranging performance. The main and reflecting anchor prototype are each implemented with a USRP X310. The main anchor transmits a total of 512 symbols, each with 330us symbol length, for CIR/TDoA estimation and ranging. The TDoA distancing is conducted by changing the relative distances between the main anchor, reflector, and tag at indoor (up to 100m TDoA) and outdoor (>100m TDoA) spaces as shown in Fig. 24.1.5. The final TDoA is estimated by a deep neural-network post-processing method [6] to achieve 1.7m median accuracy at TDoA distance of 632m when the main-anchor-to-tag distance is fixed at 64m. The accuracy improves to 1.2m median TDoA error at 632m TDoA distance when 10 packets (CIRs) are used per ranging. The tag location error is half of TDoA ranging error (thus the tag ranging error is ~0.6m) because TDoA accounts for both the distance from the main anchor to the reflector as well as the distance from the reflector to the tag. Figure 24.1.6 shows the comparison with other localization and narrowband receiver ICs. The demonstrated system presents a new long-range (up to 483m) RF localization solution with a high sensitivity (-115dBm), low power (3.9mW) and crystal-less RF receiver IC for newly emerging location-based IoT applications.

References:

[1] N. Andersen et al., "A 118-mW 23.3-GS/s Dual-Band 7.3GHz and 8.7GHz Impulse-Based Direct RF Sampling Radar SoC in 55-nm CMOS," *ISSCC*, pp. 138-139, 2017.
[2] H. G. Han et al., "A 1.9-mm-Precision 20-GHz Direct-Sampling Receiver Using Time-Extension Method for Indoor Localization," *IEEE JSSC*, vol. 52, no. 6, pp. 1509-1520, 2017.
[3] T. Redant et al., "A 40nm CMOS Receiver for 60GHz Discrete-Carrier Indoor Localization Achieving mm-Precision at 4m Range," *ISSCC*, pp. 342-343, 2014.
[4] A. T. Mariakakis et al., "Sail: Single Access Point-Based Indoor Localization," MobiCom, 2014.

2022 IEEE International Solid-State Circuits Conference (ISSCC) | 978-1-6654-2800-2/22/$31.00 ©2022 IEEE | DOI: 10.1109/ISSCC42614.2022.9731780

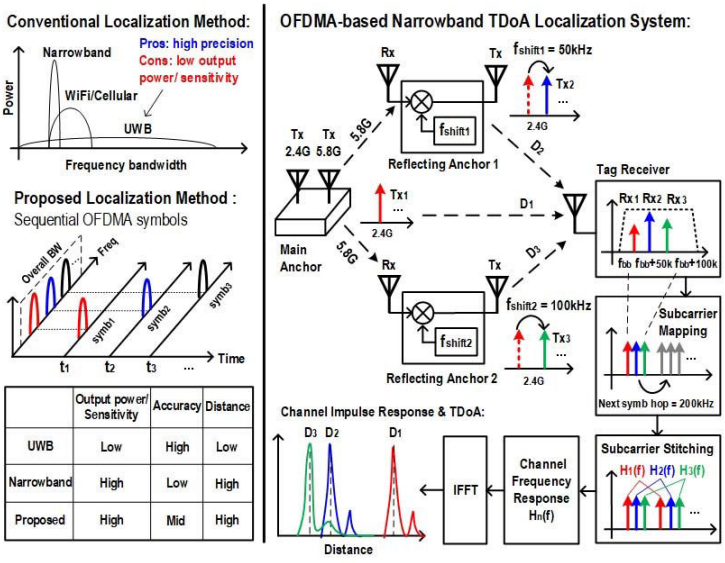

	Output power/ Sensitivity	Accuracy	Distance
UWB	Low	High	Low
Narrowband	High	Low	High
Proposed	High	Mid	High

Figure 24.1.1: Overview of proposed OFDMA-based Localization System.

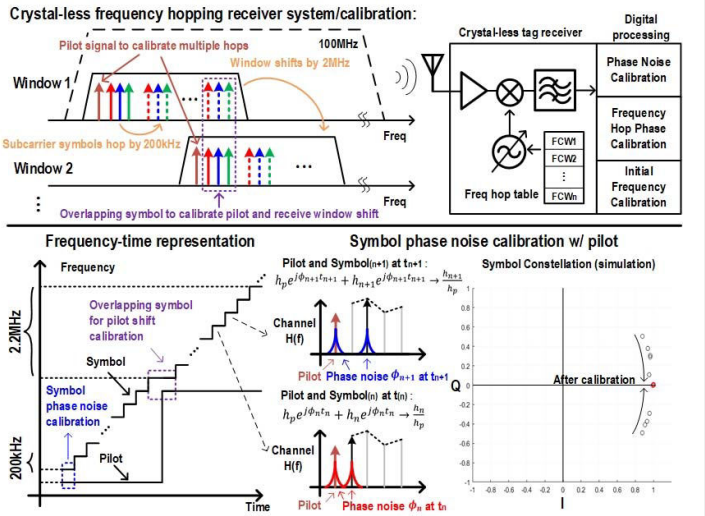

Figure 24.1.2: Crystal-less frequency-hop receiver system operation and calibration (top). Frequency-time representation of pilot and symbol (bottom, left). Illustration of symbol phase-noise calibration with pilot signal and pilot calibration with overlapping symbol (bottom, right).

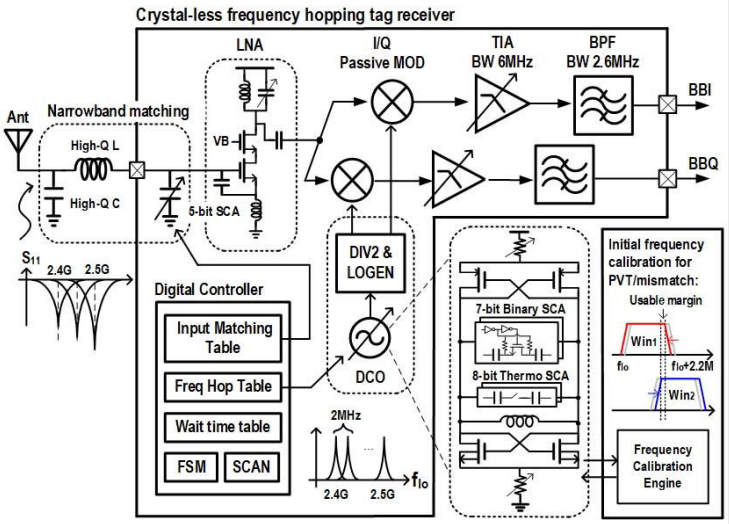

Figure 24.1.3: Crystal-less frequency-hopping tag-receiver block diagram, digital controller for DCO and input matching shifts and illustration of overlapping IF windows (right).

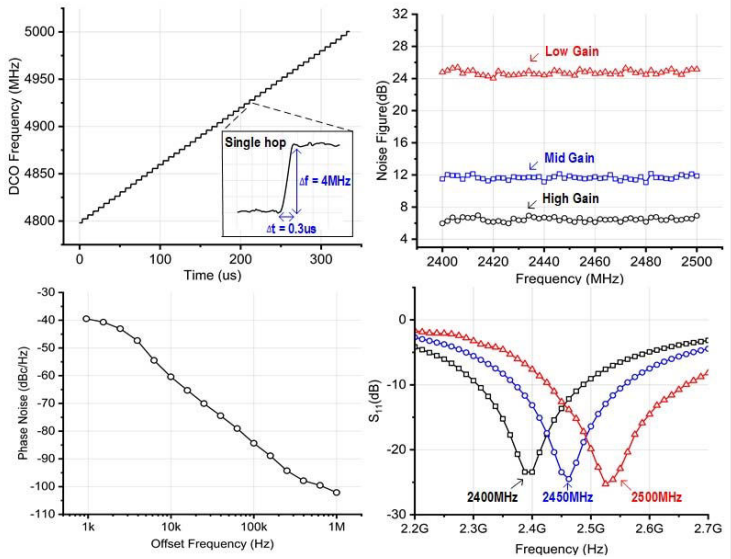

Figure 24.1.4: Measured tag receiver results: DCO frequency-hopping settling time, phase noise, receiver noise figure, and S_{11} matching.

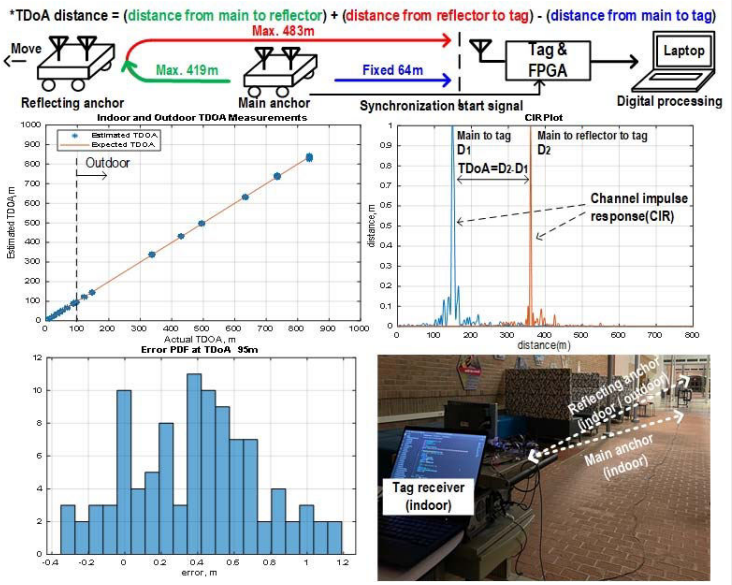

Figure 24.1.5: Ranging measurement setup and ranging result.

	This work	[1]	[2]	[3]	[5]	[7]	[8]
Standard/Modulation	TDoA/OFDMA	IR-UWB	IR-UWB	Multi-tone	BLE/GMSK	NB-IoT/OFDM	NB-IoT/OFDM
Architecture	Low-IF I/Q	Direct-sampling	Direct-sampling	Sub-sampling	Zero-IF I/Q	Zero-IF I/Q	Zero-IF I/Q
Integration Level	RXFE	TRX	RX	RX	TRX	WuRXFE	TRX
Technology	55nm CMOS	55nm CMOS	65nm CMOS	40nm CMOS	40nm CMOS	28nm CMOS	55nm CMOS
Area	0.85mm^2	8.6mm^2	6mm^2	2.93mm^2	0.89mm^2(RF)	1.08mm^2	2.23mm^2
Operation frequency	2.4-2.5GHz	7.3G/8.7GHz	4GHz	60GHz	2.4GHz	750-960MHz	450-2220MHz
Noise firugre	6.5dB	6.3dB	-	-	-	5~7dB	3.5~4.5dB
Sensitivity	-115dBm (ranging)	-	-	-	-94dBm	-109dBm	-140dBm (With repetition)
Supply voltage	0.9V	1.8/3.3V	-	-	-	0.9V	0.9V/1.1V
Rx power	3.9mW	118mW(total)	70mW(<1m)/ 320mW(2m)	195mW	5.3mW	2.1mW	11.8mW
Off-Chip matching	Yes	No	No	Yes	No	Yes	Yes
Off-chip reference	No	Yes	Yes	Yes	Yes	Yes	Yes
Ranging BW	100MHz	1.4G/1.5GHz	500MHz	2GHz	80MHz	-	-
Ranging time	181.5ms	100us	100us	20us	5.3ms	-	-
Max. range	*483m	9m	2.1m	5m	20m	-	-
Accuracy	**0.6m(380m)	1.2mm(4m)	1.9mm(47-50cm)	4mm(3.6m)	22cm	-	-

*TDoA max range is 838m, and reflector to tag max range is 483m.
**TDoA accuracy is 1.2m at 632m. Reflector to tag is 380m. The accuracy of 0.6m is from the median of 10 ranging results.

Figure 24.1.6: Performance summary and comparison to similar prior work.

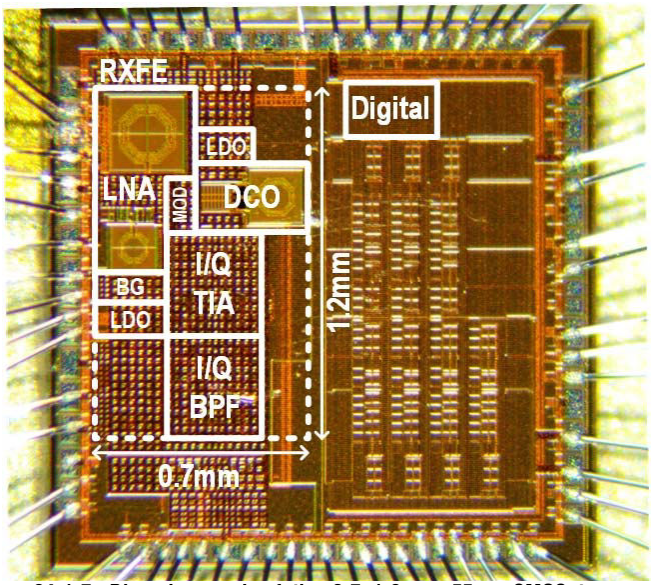

Figure 24.1.7: Die micrograph of the 0.7×1.2mm² 55nm CMOS tag receiver front-end.

Additional References:

[5] E. Bechthum et al., "A Low-Power BLE Transceiver with Support for Phase-Based Ranging, Featuring 5μs PLL Locking Time and 5.3ms Ranging Time, Enabled by Staircase-Chirp PLL with Sticky-Lock Channel-Switching," *ISSCC*, pp. 470-472, 2020.

[6] Li-Xuan Chuo et al., "RF-Echo: A Non-Line-of-Sight Indoor Localization System Using a Low-Power Active RF Reflector ASIC Tag," *MobiCom*, 2017.

[7] T. J. Odelberg et al. "A 2.1mW −109dBm NB-IoT Wake-Up Receiver," *IEEE RFIC*, pp. 235-238, 2021.

[8] P. S. Tseng et al., "A 55nm SAW-Less NB-IoT CMOS Transceiver in an RF-SoC with Phase Coherent RX and Polar Modulation TX," *IEEE RFIC*, pp. 267-270, 2019.

978-1-6654-2800-2/22/$31.00 ©2022 IEEE